Raman lasing in As_2S_3 high-Q whispering gallery mode resonators

Francis Vanier,[1,*] Martin Rochette,[2] Nicolas Godbout,[1] and Yves-Alain Peter[1]

[1]*Department of Engineering Physics, École Polytechnique de Montréal, Montréal, Quebec H3C 3A7, Canada*

[2]*Department of Electrical and Computer Engineering, McGill University, Montréal, Quebec H3A 2A7, Canada*

**Corresponding author: francis-2.vanier@polymtl.ca*

Received September 3, 2013; accepted October 17, 2013;
posted October 23, 2013 (Doc. ID 197055); published November 20, 2013

We report the first observation of a nonlinear process in a chalcogenide microresonator. Raman scattering and stimulated Raman scattering leading to laser oscillation is observed in microspheres made of As_2S_3. The coupled pump power threshold is as low as 13 μW using a pump wavelength of 1550 nm. The quality factor of the chalcogenide microresonator is also the highest ever reported with $Q > 7 \times 10^7$. © 2013 Optical Society of America

OCIS codes: (140.3945) Microcavities; (160.4330) Nonlinear optical materials; (140.3550) Lasers, Raman; (190.5650) Raman effect.

http://dx.doi.org/10.1364/OL.38.004966

The process of stimulated Raman scattering (SRS) is significant for the operation of lasers. In contrast with the electronic processes involved in typical rare-earth-doped glasses, SRS provides gain at essentially all wavelengths for which a glass is transparent. SRS and cascaded SRS are specifically important for the generation of mid-IR light required in spectroscopy and biosensing applications.

Chalcogenide glasses such as As_2S_3 and As_2Se_3 are advantageous in view of SRS emission. As_2S_3 has a high Raman gain coefficient almost 100 times that encountered in silica and has a transparency window that extends up to 6 μm in the mid-IR [1]. SRS-based lasers have already been demonstrated in As_2Se_3 fibers and microwires [2–5].

Whispering gallery mode (WGM) optical microcavities, such as microspheres, microdisks, and microtoroids, offer good possibilities for SRS emission thanks to their high quality factors and small mode volume. Threshold powers as low as 74 and 15 μW were, respectively, observed in silica microtoroids [6] and CaF_2 microdisks [7], thanks to their quality factor $Q > 10^8$. Many chalcogenide glasses WGM microcavities were reported in literature. Ga:La:S and Ga:La:S:O glass microspheres with $Q = 8 \times 10^4$ were first produced by Elliot *et al.* [8]. As_2S_3 racetrack resonators and disks, As_2S_3 and As_2Se_3 microspheres, and others were reported [9–17]. The highest Q measured was 2.3×10^6 in As_2Se_3 [12]. However, no demonstration of SRS emission has ever been reported in a chalcogenide glass WGM microcavity.

In this Letter, we present the first observation of a nonlinear process in a chalcogenide microresonator, using SRS in high-Q As_2S_3 microspheres. The microspheres used for this experiment possess the highest quality factors reported yet with chalcogenide glass. Using microspheres with loaded Q factors above 1×10^7, SRS was measured for a threshold pump power of 35 μW with a power conversion efficiency of 11%.

To fabricate the microspheres, a CO_2 laser reflow process is used, similar to the technique used for silica microspheres. For this purpose, a high purity As_2S_3 fiber provided by CorActive High-Tech is cleaned with acetone to remove the polymer cladding. The fiber is melted and pulled into a tapered fiber tip under a 3 W CO_2 laser illumination. With a diameter between 10 and 20 μm, the broken tip is melted again under CO_2 laser illumination to form a sphere from surface tension. Successive illuminations allow the production of spheres with diameters of 40 μm and above. The inset of Fig. 1 shows a typical microsphere produced with this technique.

The quality factor of spheres under test is determined from transmission spectra using evanescent coupling of a silica tapered fiber. The tapered fiber has a diameter of 2 μm. The probe laser that propagates in the tapered fiber is scanned around a wavelength of 1550 nm and the transmitted power is measured with a photodiode (Thorlabs DET01CFC). The transmission spectra are recorded over time with an oscilloscope. The time scale of the oscilloscope is converted into a wavelength scale based on the scan speed of the tunable laser. A polarization controller is used to optimize the coupling conditions. Figure 1 shows the transmitted spectrum of a resonance peak measured in a sphere having a diameter of 80 μm. The

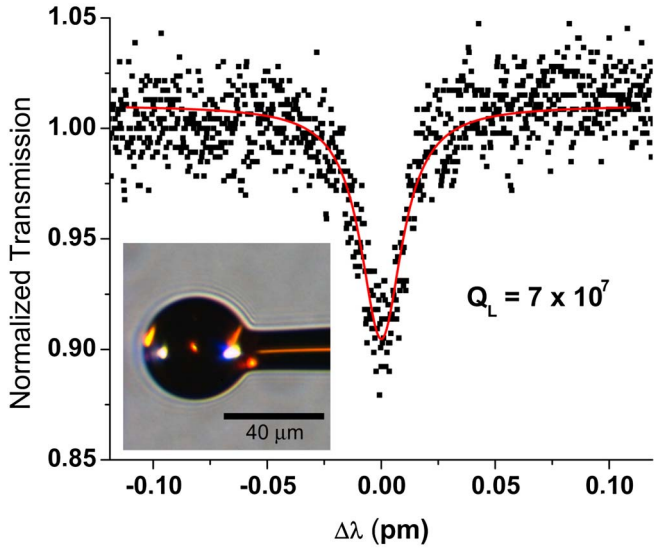

Fig. 1. Transmission spectrum of a resonance with a $Q_L = 7 \times 10^7$. Inset: micrograph of a typical microsphere produced with the laser melting process.

full width at half-maximum indicates a loaded quality factor $Q_L = 7 \times 10^7$ and an intrinsic quality factor $Q_0 = 7.2 \times 10^7$ assuming an undercoupled regime [18].

The attenuation coefficient of an As_2S_3 fiber prior to the sphere fabrication provides a lower bound on the maximum achievable quality factor. Using the attenuation value of $\alpha \approx 0.115$ m^{-1} at a wavelength of 1550 nm, the corresponding quality factor is $Q_0^{\max} = (2\pi n/\lambda\alpha) \approx 8.6 \times 10^7$. The measured quality factor indicates that the quality of the spheres produced by laser melting approaches the limit imposed by the material attenuation. Using this technique, quality factors above 10^6 and 10^7 are regularly achieved. These values are up to 100 times larger than values previously measured in an As_2S_3 microresonator and the highest reported for a chalcogenide glass [11,12,17].

With the combination of a high quality factor and a high Raman gain of $g_R \sim 4.4 \times 10^{-10}$ cm/W [1], these As_2S_3 spheres are good candidates for SRS and laser oscillation from a low pump power and with a high conversion efficiency. Figure 2 shows the experimental setup used to characterize SRS. In a first experiment, the output from an Agilent 81600B tunable laser source is evanescently coupled to the sphere with a silica tapered fiber having a diameter of 2 μm. The transmitted Raman emission is measured using an Agilent 86146B optical spectrum analyzer (OSA). The tunable laser is periodically scanned over a span of 1 nm around a central wavelength of 1549 nm. The forward Raman spectrum is measured from several scan periods by using the *Hold Max* feature of the OSA. The SRS emission is expected to be shifted 10.3 THz away from the pump and to be around 1635 nm [1,19]. A microsphere with a diameter of 71 μm is used.

Figure 3(a) shows in black the measured spectrum for an input pump power in the tapered fiber $P_{\text{in}} = 123$ μW. The forward Raman emission has a peak power of 407 nW and is located at 1636.47 nm, as expected. Only one Raman emission peak was detected at this pump power. The spectrum fluctuations are artifacts caused by the mismatched scanning synchronization of the OSA and the pump laser. The red curve shows the spectrum of a continuous wave laser line tuned to 1636.47 nm, much narrower than the resolution limit of the OSA. The red curve fits well the black one and thus the Raman laser emission spectrum from the microsphere is expected to be much narrower than the experimental acquisition profile. Forward Raman emission powers are plotted for different input pump powers in Fig. 3(b). The measurements show a linear dependency and indicate an input power threshold power $P_{\text{in}}^{\text{th}} = 61.3$ μW with a forward external conversion efficiency of 0.7%.

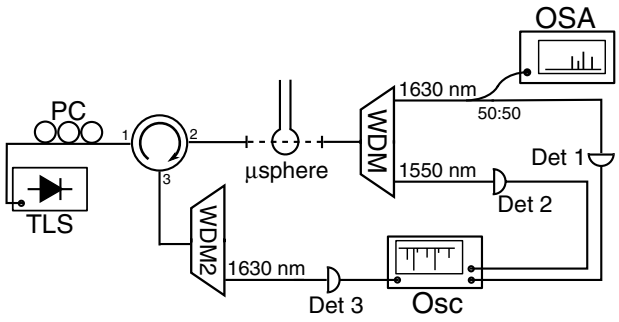

Fig. 2. Experimental setup for Raman laser emission measurements. TLS, tunable laser source; PC, polarization controler; WDM, wavelength division multiplexer; OSA, optical spectrum analyzer; Det, detector; Osc, oscilloscope.

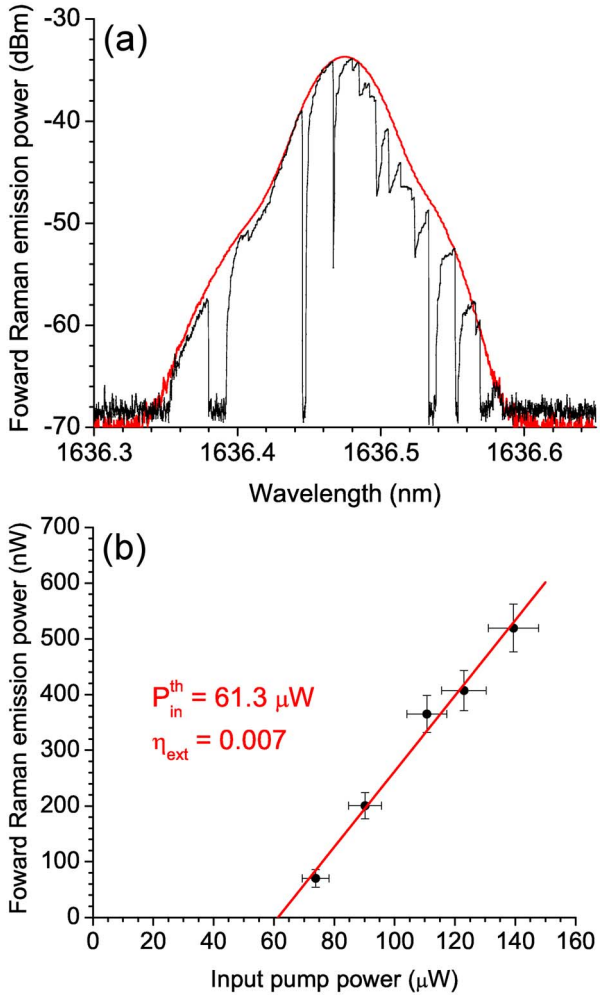

Fig. 3. (a) Raman laser emission with an input pump power of 123 μW (black curve). Superimposed (red curve) is the bandwidth-limited spectrum of a narrow cw laser, indicating that the Raman laser emission spectrum is also bandwidth-limited by the OSA. (b) Maxima of Raman emission spectra as a function of the input pump power. The Raman lasing threshold power is 61.3 μW.

To obtain the internal conversion efficiency of the process, the Raman emission in the temporal domain was measured. In a second experiment, the transmitted Raman emission and pump powers are measured with photodiodes. The backward Raman emission generated in the sphere is collected by the tapered fiber and is sent to a third photodiode. All optical powers are corrected for insertion loss of the components: PC, WDM, circulator, and tapered fiber. The pump power line is repeatedly scanned near 1552 nm over a 1 nm span and all signals are recorded with an oscilloscope. The OSA is set in zero-span mode to measure temporal profiles and allows us to identify the Raman emission wavelength. Using this setup, it is possible to plot the threshold curve in a single scan.

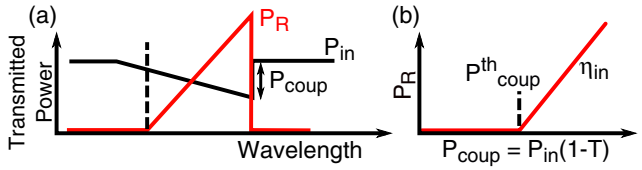

Fig. 4. Scheme of the measurements. (a) Oscilloscope view of transmitted pump and Raman emission power P_R. (b) Raman emission power against coupled pump power P_{coup} gives the coupled pump threshold power $P_{\text{coup}}^{\text{th}}$ and the internal conversion efficiency η_{in} of the Raman process. P_{in} and T are the input pump power and the transmission value, respectively.

Figure 4 illustrates the principle of the measurement. As the pump laser line shifts to gradually superimpose with a resonance from the microsphere (black line), the increase of intracavity power heats the cavity and leads to a thermal drift of the resonance, resulting in a redshift of the transmitted spectrum as shown in Fig. 4(a) [20]. At threshold (dotted line), the power coupled inside the cavity becomes large enough so that the Raman emission power (red line) turns into laser oscillation. The coupled pump power P_{coup} is related to the input pump power P_{in} in the tapered fiber by $P_{\text{coup}} = (1 - T)P_{\text{in}}$, where T is the transmission value at a particular wavelength. The Raman emission power P_R increases as long as the power inside the optical mode increases. A higher input pump power results in a longer thermal drift and a higher Raman emission power while the threshold coupled power $P_{\text{coup}}^{\text{th}}$ is maintained. By plotting the SRS emission power versus the coupled pump power, a threshold curve is obtained, as shown in Fig. 4(b). The slope of the curve is the internal conversion efficiency of the process η_{in} [21].

Figure 5 shows the transmitted pump power P_{out}, the forward Raman emission P_R^{Forw}, and the backward Raman emission P_R^{Back} in black, red, and blue, respectively, as a function of wavelength detuning. A resonance at a wavelength of 1552.5 nm with $Q_L = 3 \times 10^7$ is used. The input pump power is 49 μW. The Raman emission wavelength is 1640.7 nm and corresponds to the Raman shift. The forward and backward SRS emission start simultaneously at a wavelength detuning of 2 pm when the coupled pump power reaches threshold. The forward and backward Raman emission powers become similar as soon as the pump threshold power is exceeded, as expected.

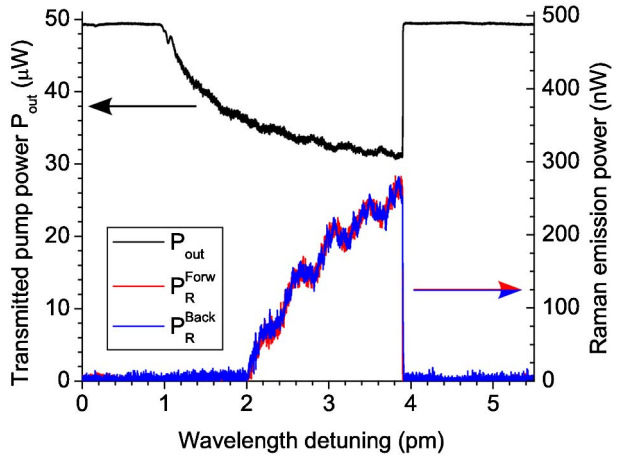

Fig. 5. Temporal domain measurements of SRS emission for an input pump power of 49 μW with transmitted pump power in black, forward Raman emission in red, and backward Raman emission in blue. Raman lasing starts at a detuning of 2 pm.

Figure 6 shows total SRS emission power as a function of the coupled pump power P_{coup} for a constant input pump power $P_{\text{in}} = 49$ μW. $P_{\text{coup}}^{\text{th}} = 12.9$ μW and an internal conversion efficiency of 10.7% are obtained. SRS emissions up to 1.1 μW were measured with $P_{\text{coup}} > 10$ μW.

The center transmittivity of the resonance used in this experiment equals 63% and leads to $P_{\text{in}}^{\text{th}} = 34.9$ μW. This threshold value is comparable to the values showed in CaF_2 disks, silica microspheres, and silica microtoroids. The transmission value also indicates a coupling quality factor $Q_c = 2.9 \times 10^8$ considering an undercoupled regime and a lossless and ideal coupling [22]. Using

$$\eta_{\text{in}} = \frac{\omega_R}{\omega_P}\frac{Q_L}{Q_c}, \tag{1}$$

where ω_P and ω_R are the pump and Raman emission frequencies, $\eta_{\text{in}} = 9.8\%$ assuming that the Raman mode quality factors are similar to the pump mode quality factors. This value agrees with the measurements and indicates an external conversion efficiency $\eta_{\text{ext}} = 2\%$. In order to improve these external conversion efficiencies, a larger coupling coefficient is needed. A possible solution is to use As_2S_3 tapered fibers, which produce better phase matching conditions compared to silica tapered fibers. The observation of higher-orders Raman emission peaks should be possible and it is currently under investigation.

To conclude, we have presented As_2S_3 microspheres fabricated using CO_2 laser melting. These spheres regularly present quality factors in the 10^6–10^7 range and up to 7×10^7, more than 2 orders of magnitude higher than reported in literature for As_2S_3 microcavities. It also represents the highest value reported for a chalcogenide

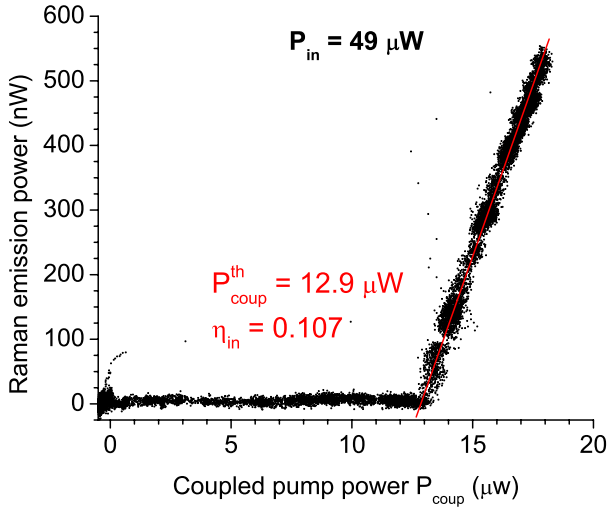

Fig. 6. Raman emission power versus coupled pump power for an input pump power of 49 μW. Raman lasing starts at 12.9 μW of coupled power with an internal conversion efficiency of 10.7%.

glass. Raman laser emissions were observed with coupled pump power down to 12.9 μW and internal conversion efficiency of 10.7%. These results show the first observation of a nonlinear process in a chalcogenide microcavity. The threshold values measured in this work are comparable to that obtained in silica and CaF_2 WGM microcavities despite smaller Q_L. Considering a transparency window up to 6 μm, As_2S_3 microspheres are good candidates for mid-IR Raman-based microlaser applications.

The authors thank CorActive High-Tech for providing chalcogenide fibers. This work was financially supported by the Fonds de recherche du Québec—Nature et Technologies (FQRNT) Equipe grant 139960.

References

1. M. Asobe, T. Kanamori, K. Naganuma, H. Itoh, and T. Kaino, J. Appl. Phys. **77**, 5518 (1995).
2. R. Ahmad and M. Rochette, Appl. Phys. Lett. **101**, 101110 (2012).
3. R. Ahmad and M. Rochette, Opt. Lett. **37**, 4549 (2012).
4. S. D. Jackson and G. Anzueto-Sánchez, Appl. Phys. Lett. **88**, 221106 (2006).
5. M. Bernier, V. Fortin, N. Caron, M. El-Amraoui, Y. Messaddeq, and R. Vallée, Opt. Lett. **38**, 127 (2013).
6. T. J. Kippenberg, S. M. Spillane, D. K. Armani, and K. J. Vahala, Opt. Lett. **29**, 1224 (2004).
7. I. S. Grudinin and L. Maleki, Opt. Lett. **32**, 166 (2007).
8. G. R. Elliott, D. W. Hewak, G. Senthil Murugan, and J. S. Wilkinson, Opt. Express **15**, 17542 (2007).
9. J. Hu, N. Carlie, L. Petit, A. Agarwal, K. Richardson, and L. Kimerling, Opt. Lett. **33**, 761 (2008).
10. C. Grillet, S. N. Bian, E. C. Magi, and B. J. Eggleton, Appl. Phys. Lett. **92**, 171109 (2008).
11. J. Hu, N. Carlie, N.-N. Feng, L. Petit, A. Agarwal, K. Richardson, and L. Kimerling, Opt. Lett. **33**, 2500 (2008).
12. D. H. Broaddus, M. A. Foster, I. H. Agha, J. T. Robinson, M. Lipson, and A. L. Gaeta, Opt. Express **17**, 5998 (2009).
13. M. E. Solmaz, D. B. Adams, W. C. Tan, W. T. Snider, and C. K. Madsen, Opt. Lett. **34**, 1735 (2009).
14. G. R. Elliott, G. Senthil Murugan, J. S. Wilkinson, M. N. Zervas, and D. W. Hewak, Opt. Express **18**, 26720 (2010).
15. F. Luan, E. Magi, T. Gong, I. Kabakova, and B. J. Eggleton, Opt. Lett. **36**, 4761 (2011).
16. P. Wang, G. Senthil Murugan, G. Brambilla, M. Ding, Y. Semenova, Q. Wu, and G. Farrell, IEEE Photon. Technol. Lett. **24**, 1103 (2012).
17. P. Wang, M. Ding, T. Lee, G. Senthil Murugan, L. Bo, Y. Semenova, Q. Wu, D. Hewak, G. Brambilla, and G. Farrell, Appl. Phys. Lett. **102**, 131110 (2013).
18. F. Vanier, C. La Mela, A. Hayat, and Y.-A. Peter, Opt. Express **19**, 23544 (2011).
19. A. Schulte, C. Rivero, K. Richardson, K. Turcotte, V. Hamel, A. Villeneuve, T. Galstian, and R. Vallée, Opt. Commun. **198**, 125 (2001).
20. T. Carmon, L. Yang, and K. J. Vahala, Opt. Express **12**, 4742 (2004).
21. T. J. Kippenberg, S. M. Spillane, B. Min, and K. J. Vahala, IEEE J. Sel. Top. Quantum Electron. **10**, 1219 (2004).
22. S. M. Spillane, T. J. Kippenberg, O. J. Painter, and K. J. Vahala, Phys. Rev. Lett. **91**, 043902 (2003).